Cherns, L., et al., 2022, Correlative tomography of an exceptionally preserved Jurassic ammonite implies hyponome-propelled swimming: Geology, https://doi.org/10.1130/G49551.1

Correlative tomography of exceptionally preserved Jurassic ammonite implies hyponome-propelled swimming

Lesley Cherns*, Alan R. T. Spencer, Imran A. Rahman, Russell J. Garwood, Chris Reedman, Genoveva Burca, Martin J. Turner, Neville T. J. Hollingworth, and Jason Hilton

*E-mail: cherns@cardiff.ac.uk

Material

A single specimen of *Sigaloceras* (*Catasigaloceras*) *enodatum* Nikitin, 1881 from the Lower Callovian (Calloviense Biozone) Kellaways Sand Member (Fig. S1) of Colne Gravel, Claydon Pike pit, Fairford, Gloucestershire, UK (site now flooded). WGS 30U 587216.566 5728069.106. The internal mold has been split away from the shell, with two halves of the shell being retained in two blocks of consolidated matrix. The relatively small specimen is mature, as it shows approximation of the last two sutures and uncoiling of the umbilical seam, while loss of ornament on the body chamber is consistent with a macroconch (Callomon, 1955; Fig. S2). A shallow anterior lateral sinus apparent on the mold (Mironenko 2014; Fig. 1) is distinct from the deep lateral sinus of some ammonoids (Doguzhaeva and Mutvei 1996). The specimen is deposited at the National Museum Wales, Cardiff. Accession no. NMW.2002.69G.1.

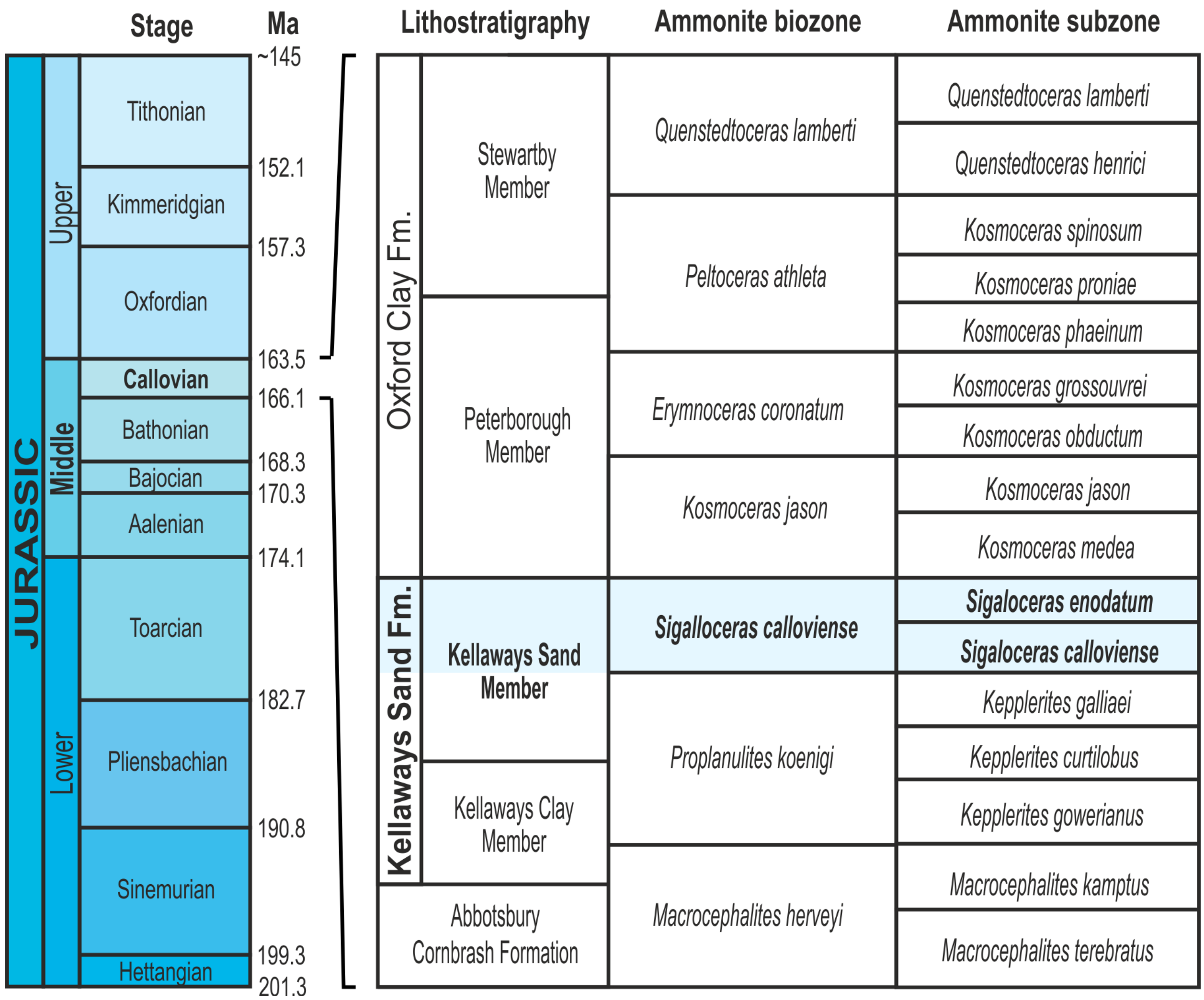

Fig. S1. Stratigraphic framework for the Jurassic of the UK. Modified from Spencer et al. (2017).

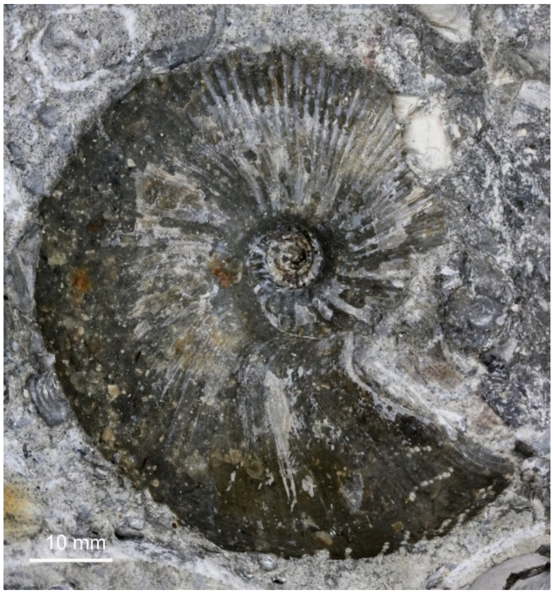

Fig. S2. Ammonite block (counterpart); note uncoiling of umbilical seam and loss of ornament on body chamber.

Geological setting

The Claydon Pike pit site consists of poorly cemented, calcareous sands, including laterally impersistent calcareous sandstones, and abundant shelly lenses and diagenetic sandy limestone concretions that have diverse, molluscan-rich assemblages. This unit represents a period of basinward, transgressive spread of coarse siliciclastic facies close to the edge of the London Brabant massif, deposited in shallow and periodically high energy environments. Within the concretion containing the *S. enodatum* macroconch, many shells are disarticulated and fragmented, and they are closely packed, locally imbricated and winnowed in a micritic to microsparitic, sandy matrix with abundant woody debris. Winnowed shelly accumulates created by storm disturbance affected the shelly benthos, but ammonites were also buried rapidly under prograding shell sand ripples. The *S. enodatum* specimen shows no evidence of prolonged exposure (e.g., scavenging, shell encrustation, reworking of sediment fill), nor of exhumation from elsewhere and re-deposition, as the sedimentary fill in the apical parts of the body-chamber is the same as the matrix of the concretion.

Methods

The internal mold was photographed using both transmitted and reflected photography in artificial white light with a Nikon D700. Images were color corrected and balanced using GIMP 2.8 (https://www.gimp.org). Scanning electron microscopy (SEM) was undertaken using an environmental chamber SEM at the Natural History Museum, London. In addition, energy dispersive X-ray spectroscopy (EDX) was performed using a Cambridge Instruments SEM in the Department of Earth Sciences, Cardiff University.

Neutron tomography was performed at the IMAT beamline (Burca et al., 2018) of ISIS Neutron and Muon Spallation Source, UK, using an optical camera box equipped with a Zyla sCMOS 4.2 Plus camera (www.andor.com), 135 mm lens from Nikon, a 45 degree optical mirror and a 6LiF / ZnS scintillator with a thickness of 80 µm. For a field-of-view of 120×120 mm^2, an effective pixel size of 58 µm was used. A total of 1801, 30 second projections were acquired over 360° rotation. Projections were reconstructed as two-dimensional slices using Octopus Imaging Software (https://octopusimaging.eu) (Rahman et al., 2018). X-ray microtomography was undertaken using a Nikon Metrology XTek XT H 225 at the University of Manchester, UK, with a 0.5 mm copper filter, 145 kV voltage and 85 µA current, capturing 6000 projections on a 3192×2296 detector. Projections were reconstructed using Nikon Metrology NV’s XT 5.1.4.3 software (https://www.nikonmetrology.com). The resultant image stack (3190×3192×1151) had a voxel size of 0.0196 mm.

A combined three-dimensional model was created in DragonFly 4.1 (https://www.theobjects.com/dragonfly/index.html). Both the X-ray and neutron tomography datasets were imported into the software. The X-ray microtomography dataset, which reveals the internal and external shell structure at high resolution (19 µm voxels), was used to register and align the neutron tomography dataset in three dimensions, which is of lower resolution (58 µm voxels. This allowed both sets of data to be viewed together. Attenuation mechanisms differ between the incident radiations, picking out different details. Thus, by combining areas within the 3D space of differing attenuation, either X-ray or neutron, we were able to individually mask regions of interest (ROIs). These regions were volume rendered by the software as manipulable false-colour 3D objects. The ROIs were subsequently processed to remove any islands of 9–50 voxels in total number using the 6-connected method. Contour meshes were generated from these ROI's using a threshold of 50 and linear sampling in the x, y, and z of either 1, 2, or 4 (dependent of the initial size of the ROI). The resultant meshes were then iteratively smoothed five times, using laplacian smoothing, before being exported to an STL format file as binary. Figures and videos of the model were generated in Blender 2.82 (https://www.blender.org). Data generated during this study are available on Zenodo: https://doi.org/10.5281/zenodo.5118538

Photographs were acquired with a Nikon D90 digital single-lens reflex camera. A total of 143 photographs were taken at a resolution of 4288×2848 pixels. Photographs were masked with GIMP 2.8 to remove the background surrounding the specimen using the fuzzy, scissor and lasso select tools, then exported as PNG files. Photogrammetry was performed using Agisoft Metashape 1.5.3 (https://www.agisoft.com), importing masks from the alpha png layer. A sparse point cloud was then generated, incorrectly positioned points manually cleaned, a dense cloud created and then meshed and exported in .ply format.

Movie S1. Virtual reconstruction of *S. enodatum*. Movie available at:

Ammonite_video_29Sep_21.mkv

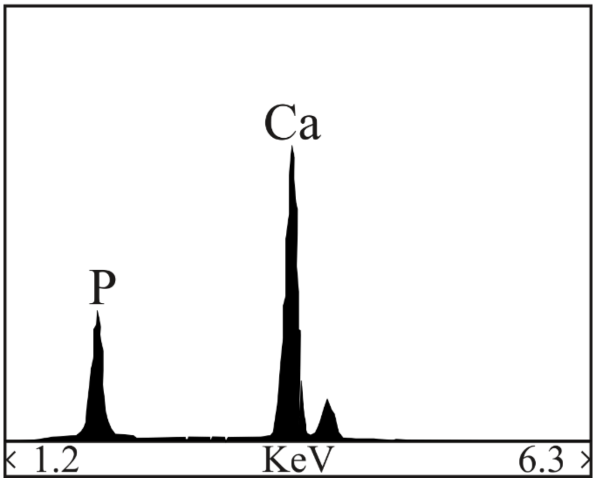

Figure S3. Energy dispersive X-ray spectrum of siphuncle of *S. enodatum*, indicating apatitic composition of dark fill.

REFERENCES CITED

Burca, G., Nagella, S., Clark, T., Tasev, D., Rahman, I.A., Garwood, R.J., Spencer, A.R.T., Turner, M.J., and Kelleher, J.F., 2018, Exploring the potential of neutron imaging for life sciences on IMAT: Journal of Microscopy, v. 272, p. 242–247, https://doi.org/doi:10.1111/jmi.12761.

Callomon, J.H., 1955, The ammonite succession in the Lower Oxford Clay and Kellaways beds at Kidlington, Oxfordshire, and the zones of the Callovian Stage: Philosophical Transactions of the Royal Society B, v. 239, p. 215–264, https://doi.org/10.1098/rstb.1955.0010.

Rahman, I.A., Garwood, R.J., Burca, G., and Spencer, A.R.T., 2018, Applying neutron tomography to exceptionally preserved fossils with poor X-ray contrast: STFC ISIS Neutron and Muon Source, https://doi.org/10.5286/ISIS.E.RB1810821.

Spencer, A.R.T., Garwood, R.J., Rees, A.R., Raine, R.J., Rothwell, G.W., Hollingsworth, N.T.J., and Hilton, J., 2017, New insights into Mesozoic cycad evolution: An exploration of anatomically preserved Cycadaceae seeds from the Jurassic Oxford Clay biota: PeerJ, v. 5, e3723, https://doi.org/10.7717/peerj.3723.